Available online at www.sciencedirect.com

SCIENCE DIRECT®

International Journal of Mass Spectrometry 254 (2006) 85–93

www.elsevier.com/locate/ijms

Chemical ionization reaction time-of-flight mass spectrometry: Multi-reagent analysis for determination of trace gas composition

Robert S. Blake, Kevin P. Wyche, Andrew M. Ellis, Paul S. Monks *

Department of Chemistry, University of Leicester, Leicester LE1 7RH, UK

Received 12 April 2006; received in revised form 18 May 2006; accepted 24 May 2006

Abstract

Chemical ionization reaction mass spectrometry (CIRMS) is applied for the first time to a range of organic gases with a variety of functional groups. This technique, recently developed, is an extension to proton transfer reaction-mass spectrometry (PTR-MS) using a greater variety of chemical ionization reagents in the ionization process. Clean sources of the reagents H_3O^+, NH_4^+, NO^+ and O_2^+ have been obtained without any mass pre-selection. The reactions of these reagent ions with a range of test VOCs are found to be rapid, with the chemistry generally paralleling that observed previously with selected ion flow tube measurements, although with some important differences. CIRMS is shown to be a more versatile technique than conventional PTR-MS with the potential for rapid multi-reagent analysis of chemical mixtures.

Keywords: Chemical ionization; CIRMS; PTR-MS; Proton-transfer

1. Introduction

Proton transfer reaction-mass spectrometry (PTR-MS) is now seeing widespread use as a tool for detecting and quantifying trace volatile organic compounds (VOCs) in the gas-phase. Applications have already been found in areas as diverse as atmospheric composition and pollution studies [1], aroma analysis [2] and medical science through breath analysis [3–5]. The range of applications is likely to broaden as more research teams recognize the strengths of this analytical technique.

The *modus operandi* of PTR-MS is the chemical ionization, by proton transfer, of a gas sample inside a drift-tube. The fixed length of the drift-tube provides a fixed reaction time for the ions as they pass along the tube: the reaction time can be measured or it can be calculated from ion transport properties. If the proton donor is present in large excess over the acceptor molecules, then a measurement of the ratio of donor/protonated acceptor ion signals allows the concentration of the acceptor molecules to be calculated. This calculation is straightforward and requires only the rate constant for proton transfer, which may be available experimentally or which can readily be estimated using tried and tested theoretical models [6].

Proton transfer is a relatively soft ionization technique [1]. This property is beneficial when analysing complex mixtures, since excessive fragmentation will complicate, or even prevent, compound identification. However, this simplification comes at the cost of being unable to distinguish between isobaric molecules. In addition, while proton transfer is an effective way of ionizing many organic molecules, it is not universally successful. The most commonly used proton donor in chemical ionization is H_3O^+ [1]. This ion is also the main proton source for PTR-MS, since it can be generated relatively cleanly and simply in the gas-phase without any need for mass pre-selection. However, H_3O^+ will not protonate a number of hydrocarbons, particularly small alkanes and alkenes such as ethene, and also a number of chlorofluorocarbons. In addition, it has limited utility for ionizing small inorganic gases because of their often unfavourable proton affinities.

PTR-MS has much in common with selected ion flow tube mass spectrometry (SIFT-MS). An important difference between the two techniques is that in SIFT-MS mass pre-selection of ions is employed. Extensive work on the ion–molecule chemistry in SIFT reactors has been carried out by Smith and Španel and co-workers [7–14]. This research team have explored the chemistry not only of H_3O^+, but also of other chemical ionization (CI) reagents such as NO^+ and O_2^+. Like H_3O^+, these alternative ions tend to react rapidly with most organic molecules. Although

---

* Corresponding author. Tel.: +44 1162522141; fax: +44 1162523789.
E-mail address: P.S.Monks@le.ac.uk (P.S. Monks).

1387-3806/$ – see front matter © 2006 Elsevier B.V. All rights reserved.
doi:10.1016/j.ijms.2006.05.021

H_3O^+ is ideal for many applications, NO^+ and $O_2{}^+$ have also been shown to have their uses. For example, NO^+ is a relatively soft ionizer, like H_3O^+, but the ionization occurs mainly through either charge transfer or hydride ion transfer, thereby yielding different ion products. $O_2{}^+$ is found to be a more aggressive CI reagent and is often suitable for detecting those species which cannot be detected by proton transfer.

The ability to switch readily between CI reagents such as H_3O^+, NO^+ and $O_2{}^+$, gives SIFT-MS an added dimension which PTR-MS, until recently, did not possess. However, in a recent communication we showed how a PTR-MS instrument could be adapted to operate with NO^+ as the CI reagent [15]. As with H_3O^+, generation of NO^+ could be achieved cleanly without any need for mass pre-selection. Furthermore, it is trivial and quick to switch between NO^+ and H_3O^+ as the ion source. The aim in that initial work was to show that, by using NO^+ instead of H_3O^+, it was possible to distinguish between isobaric aldehydes and ketones. The basic role of the NO^+ ion was to introduce a degree of ion fragmentation and complexation that provided a characteristic mass spectral 'fingerprint' of a specific aldehyde or ketone. Consequently, NO^+ could be used to allow speciation of isobaric species on the same instrument used for conventional PTR-MS work. The instrument employed is a homemade device equipped with a radioactive ion source and a time-of-flight mass spectrometer. Because we are not restricted to proton-donating CI reagents, we called this technique chemical ionization reaction mass spectrometry, or CIRMS for short.

In this paper we explore the CIRMS technique in more detail. A range of volatile compounds is employed with representatives from a number of organic functional groups, including alkenes, aromatic hydrocarbons, alcohols, aldehydes, ketones, nitriles and esters. In addition, a wider range of CI reagents is employed, which now includes $O_2{}^+$ and $NH_4{}^+$ alongside NO^+. Potentially, this array of CI reagents should put CIRMS and SIFT-MS on the same footing in terms of being able to select the best CI reagent for a specific task. The cleanliness of the CI reagent ion production, the characteristic reaction products under typical CIRMS reaction conditions and potential applications of this wider range of CI reagents are discussed. In addition, an important part of this study is a comparison with the extensive body of SIFT-MS work by Smith and Španel, in order to determine if the chemistry and rate data established under SIFT-MS conditions is also applicable in CIRMS.

2. Experimental

The instrument used for this study is essentially the same as the PTR-MS instrument developed in our laboratory and which has been described in detail elsewhere [16]. Briefly, the instrument consists of an ion source containing a 44.4 MBq ^{241}Am α-particle source, which is used to ionize the desired CI reagent, normally in a buffer gas (e.g., N_2). This source is based on a design developed by Hanson et al. [17]. The reagent ions are drawn into a 10 cm long drift-tube where they mix and react with the analyte gas. Unreacted and product ions move downstream guided by a 2.7 kV potential difference along the drift-tube. At the end of the drift-tube is a 200 μm exit aperture, through which ions can leave and enter the ion focusing optics of a reflectron time-of-flight mass spectrometer.

H_3O^+ ions were generated from saturated water vapour carried along by high purity nitrogen (BOC 99.998%). The source gas for the NO^+ reagent ions was a 600 ppmv mixture of NO in nitrogen (BOC α-spectraseal). Cylinders of pure O_2 (BOC Special Gases N5.0) and NH_3 (BOC Special Gases, MS grade) were used to produce $O_2{}^+$ and $NH_4{}^+$. The reagent gas mixtures (except water/N_2) were passed through coils cooled by dry ice to remove H_2O. The tendency of the reagent ions to form clusters, which can interfere with some reactions [9], was reduced (<5%) by operating at an E/N of 165 Td, where E is the electric field and N is the gas number density.

The analytes employed in this work are listed in Table 1, along with their proton affinities, the supplier and the minimum sample purity. Analyte samples were continuously flowed into the upstream part of the drift-tube by entrainment in flowing dry nitrogen (BOC 99.998%). As all the analytes except 1-butene are liquids at room temperature, a head-space extraction was used in which the carrier gas was passed over the liquid sample in a sealed vessel at a flow rate of 275 sccm. The drift-tube, CI reagent and analyte gas inlet lines were maintained at a temper-

Table 1
Analytes employed in this work

Item	PA[a] (kJ mol^{-1})	IE[b] (eV)	Purity	Source
Acetaldehyde	769.0	10.2291 ± 0.0007	99%	Sigma–Aldrich
Acetone	812.1	9.703 ± 0.006	>95%	Sigma–Aldrich
Acetonitrile	779.1	12.20 ± 0.01	>95%	Sigma–Aldrich
Benzene	750.2	9.24378 ± 0.00007	>95%	Sigma–Aldrich
1-Butene	746.8	9.55 ± 0.06	1 ppmv/N_2	BOC Special Gases
Ethanol (anhydrous)	776.6	10.48 ± 0.07	>98%	Sigma–Aldrich
Ethyl acetate	835.7	10.01 ± 0.05	>95%	Fisher Scientific
Hexanal	–	9.72 ± 0.05	98%	Sigma–Aldrich
Methacrolein	808.8	9.92	95%	Sigma–Aldrich
Methyl benzoate	850.5	9.32 ± 0.04	>95%	Sigma–Aldrich
Methyl vinyl ketone	834.7	9.65 ± 0.02	95%	Sigma–Aldrich
Toluene	784.1	8.828 ± 0.001	>95%	Fisher Scientific

[a] PA: proton affinity. Where available data have been taken from Ref. [20].
[b] IE: adiabatic first ionization energy (taken from Ref. [20]).

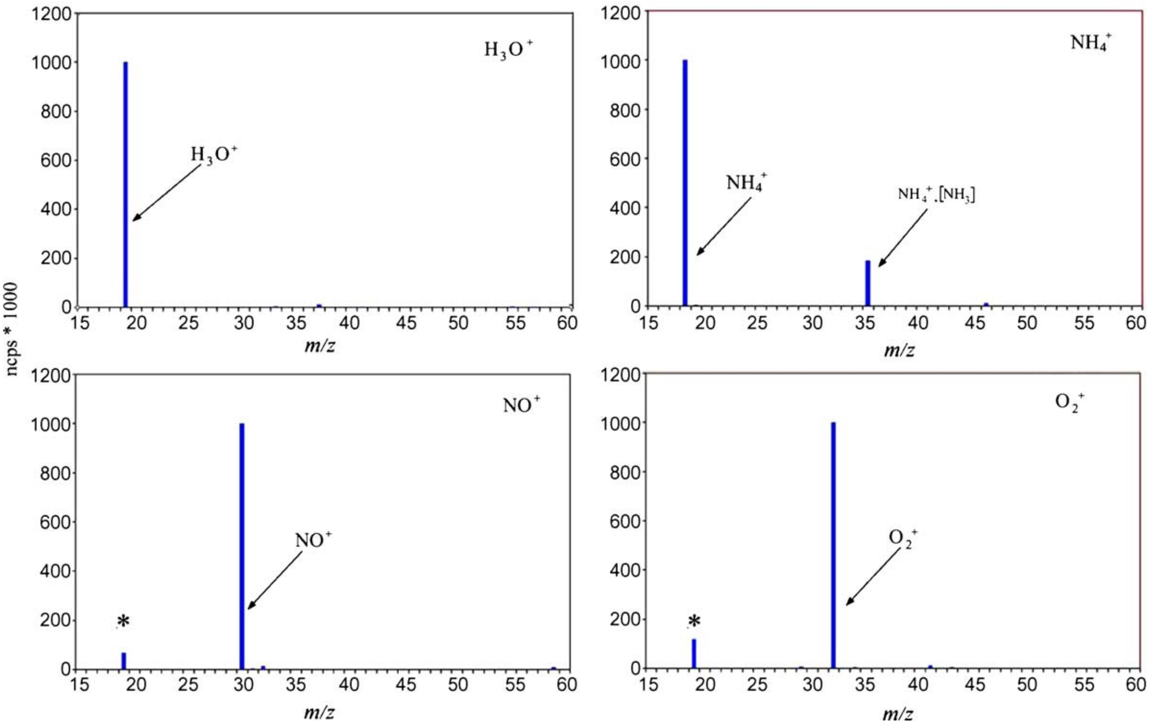

Fig. 1. Mass spectra obtained for the four reagent ion sources. For these scans no analyte gas was added. Traces of H_3O^+ contamination, labelled with an asterisk, are present in the O_2^+ and NO^+ spectra.

ature of 40 °C to minimize gas condensation on the inlet and drift-tube walls. A constant temperature drift-tube allows constant reaction conditions for the chemical ionization.

3. Results

The findings for H_3O^+ will first be described and then NH_4^+, NO^+ and O_2^+ in turn. Examples of the spectral data are shown in Figs. 1 and 2, which show, respectively, the mass spectra in the absence of any analyte gas (ion source mass spectrum) and the mass spectra obtained for an example analyte, hexanal, with all four CI reagents. In the analysis and presentation of the mass spectral data, as shown in Fig. 2, it should be noted that each analyte spectrum has first been processed by subtracting background contributions obtained from blank runs (analyte gas flow off but CI reagent flow on).

3.1. Reactions of H_3O^+

The products from the reactions of H_3O^+ with all the analyte gases are summarized in Table 2. All of the analytes possess higher proton affinities than H_2O, as can be seen from Table 1, and so rapid proton transfer occurs in each case. The products of proton transfer from H_3O^+ to VOCs have been

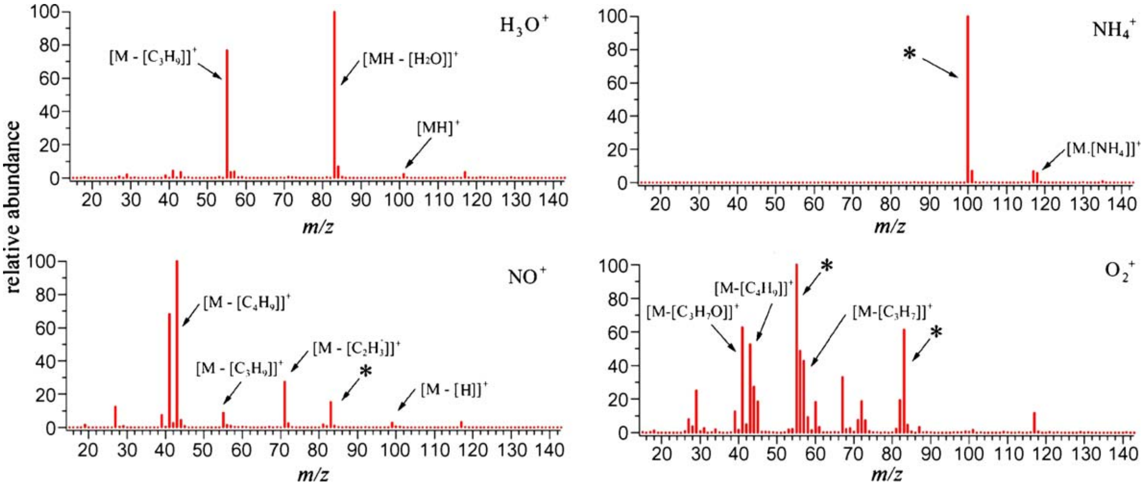

Fig. 2. Mass spectra of hexanal obtained using H_3O^+, NH_4^+, NO^+ and O_2^+ CI reagent ions. Trace H_3O^+ contamination are labelled with an asterisk.

Table 2
Product distributions from the reaction of H_3O^+ with a range of analytes at *E*/*N* = 165 Td

Compound	M	Product ion	*m*/*z*	Relative abundance
Acetaldehyde	C_2H_4O	$((M–H)H_2O))^+$	61	26
		MH^+	45	47
		$(M(–H))^+$	43	20
		Not identified	41	6
		Not identified	39	1
Acetone	C_3H_6O	MH^+	59	100
Acetonitrile	C_2H_3N	MH^+	42	100
Benzene	C_6H_6	MH^+	79	100
1-Butene	C_4H_8	MH^+	57	25
		$(M(–CH_3))^+$	41	30
		$(M(–C_2H_3))^+$	29	45
Ethanol	C_2H_6O	MH^+	47	93
		$(MH–(H_2O))^+$	29	7
Ethyl acetate	$C_4H_8O_2$	MH^+	89	5
		$(M–(C_2H_3))^+$	61	74
		$(M–(C_2H_3O))^+$	43	21
Hexanal[a]	$C_6H_{12}O$	$(MH–(H_2O))^+$	83	57
		$(M–(C_3H_9))^+$	55	43
Methacrolein	C_4H_6O	MH^+	71	87
		$(M–(C_2H_3))^+$	43	9
		$(M–(CHO))^+$	41	4
Methyl benzoate	$C_8H_8O_2$	MH^+	137	88
		$(M–(CH_3O)^+$	105	12
Methyl vinyl ketone	C_4H_6O	MH^+	71	95
		$(MH–(C_2H_4))^+$	43	5
Toluene	C_7H_8	MH^+	93	100

[a] Trace amounts <2% of MH^+ and carbonyl fragmentation products of *m*/*z* 57, 43, 41, 29 are also observed (see for example Fig. 2 in Ref. [15]).

extensively studied elsewhere, both by PTR-MS [1] and by SIFT-MS [7–14], so an extensive discussion is not required here.

Briefly, for all the compounds investigated in the present work SIFT-MS has been found to yield only the protonated parent species. Under CIRMS conditions employed in the present study, the same ions dominate in most cases, but there is now also a moderate degree of fragmentation for some of the compounds. The only dramatic differences were found for ethyl acetate and hexanal, where protonation leads to predominantly dissociated product ions. The differences between the SIFT-MS findings and the current work are attributed to differences in ion collision energies, which are greater in the case of CIRMS (see Section 4 later). Some of these differences were also reported in the PTR-MS work of Warneke et al. [18]. For all compounds except ethanol there is good agreement with the data in Ref. [18], the small differences for acetone and hexanal being attributable to the slightly larger values of *E*/*N* used in the present work. For ethanol, Warneke et al. [18] found a 50:50 ratio for *m*/*z* 47 and 29 compared to 93:7 in this work (see Table 2), which is anomalous given the ratios of *E*/*N* in both sets of work and merits further investigation.

3.2. Reactions of NH_4^+

Protonated ammonia has been used previously in PTR-MS, most notably in some of the early studies by Lindinger et al. [1]. The reactions of NH_4^+ ions with VOCs have also been investigated previously by SIFT-MS [19]. As ammonia possesses a much higher proton affinity than water, 854 instead of 691 kJ mol^{-1} [20], it can only be used to ionize a much narrower set of molecules than H_3O^+. However, this selectivity could be beneficial if two isobaric species are present in a gas mixture, when only one is able to accept a proton from NH_4^+. Lindinger et al. discussed just such an example in an early PTR-MS study, namely the use of NH_4^+ to discriminate between pinene and 2-ethyl-3,5-dimethylpyrazene (only pyrazene has a proton affinity exceeding that ammonia) [1]. The reactions of NH_4^+ ions are included here primarily to show the versatility of the CIRMS technique as a multi-reagent source.

Fig. 1 includes a mass spectrum obtained with the CI precursor, neat ammonia, but with no added analyte. The radioactive ion source acts as a relatively clean source of NH_4^+, the only significant contaminant being the protonated dimer ion, $NH_4^+(NH_3)$. The relative abundance of the dimer would almost certainly be reduced by diluting the ammonia in a flow of nitrogen carrier gas, but this was not explored in the current work.

Table 3 summarizes the products obtained from the reactions of NH_4^+ with the various analytes investigated in the present work. On the basis solely of the proton affinities listed in Table 1, no proton transfer reactions between NH_4^+ and any of the analyte molecules are expected. The mass spectra confirm this to be the

Table 3
Product distributions from the reaction of NH_4^+ with a range of analytes at *E*/*N* = 165 Td

Compound	M	Product ion	*m*/*z*	Relative abundance
Acetaldehyde	C_2H_4O	None observed		
Acetone	C_3H_6O	$(M\cdot(NH_4))^+$	76	91
		$[(M\cdot(NH_4))\cdot(NH_3)]^+$	93	9
Acetonitrile	C_2H_3N	$(M\cdot(NH_4))^+$	59	95
		$[(M\cdot(NH_4))\cdot(NH_3)]^+$	76	5
Benzene	C_6H_6	None observed		
1-Butene	C_4H_8	None observed		
Ethanol	C_2H_6O	None observed		
Ethyl acetate	$C_4H_8O_2$	$(M\cdot(NH_4))^+$	106	95
		$[(M\cdot(NH_4))\cdot(NH_3)]^+$	123	5
Hexanal	$C_6H_{12}O$	$(M\cdot(NH_4))^+$	118	100
Methacrolein	C_4H_6O	$(M\cdot(NH_4))^+$	88	91
		$[(M\cdot(NH_4))\cdot(NH_3)]^+$	105	9
Methyl benzoate	$C_8H_8O_2$	$(M\cdot(NH_4))^+$	154	90
		$[(M\cdot(NH_4))\cdot(NH_3)]^+$	171	10
Methyl vinyl ketone	C_4H_6O	$(M\cdot(NH_4))^+$	88	95
		$[(M\cdot(NH_4))\cdot(NH_3)]^+$	105	5
Toluene	C_7H_8	None observed		

case. Benzene, toluene, 1-butene and ethanol show no reaction at all with NH_4^+. However, the majority of the molecules do react with NH_4^+ to give association complexes, i.e.,

$$M + NH_4^+ \rightarrow M \cdot (NH_3)^+ + H \tag{1}$$

Association products from the cluster ions $NH_4^+(NH_3)$ are also seen for some of the analytes and reflect the substantial abundance of $NH_4^+(NH_3)$. There are potential applications for this phenomenon in the decongestion of spectra.

3.3. Reactions of NO^+

Španel and Smith have provided an extensive discussion of the reactions of NO^+ with a wide variety of VOCs [7–14]. The first ionization energy of NO is 9.6 eV [20], which limits non-dissociative charge transfer to those analytes with relatively low ionization energies. For other molecules alternative processes may occur, including hydride ion transfer and/or ion association reactions.

Table 4 details the observed products from reactions of NO^+ in the present work. There are two main differences between the CIRMS findings and previous SIFT-MS work. First, there is tendency for a greater degree of fragmentation and a wider range of fragment ions in the CIRMS experiments. For example, ethanol has been found to undergo only hydride ion transfer in SIFT-MS to yield the CH_3CHOH^+ ion [8]. In contrast, while hydride ion transfer also dominates in CIRMS, another significant product is CH_2OH^+, which is presumably formed by the methyl anion transfer reaction

$$NO^+ + CH_3CH_2OH \rightarrow CH_2OH^+ + CH_3NO \tag{2}$$

The other notable difference is the almost complete lack of any association complexes with NO^+, which is in marked contrast to the findings from SIFT-MS, where $M{\cdot}NO^+$ ions are common for a wide variety of organic molecules. The only exception to this statement for the entire set of molecules investigated in this work is 1-butene, where a substantial association complex peak is seen, as shown in the central panel of Fig. 3. Acetonitrile appears also to undergo some degree of association (see Table 4). However, unlike the case of 1-butene, it is the hydride ion product, not the neutral that forms the association complex.

The differences between SIFT-MS and CIRMS can be attributed to the higher collision energy in the latter (see also Section 4 later). This is reasonable in explaining not only the increased number of fragmentation products seen in some cases, but also the absence of the association complexes with NO^+. For example, Smith and co-workers have reported 100% production of $CH_3CN{\cdot}NO^+$ from the reaction of acetonitrile with NO^+ [9], while in the case of benzene the association product formed 15% of the overall ion products, the remainder being benzene cation [13]. In our CIRMS experiments only the benzene cation is observed. This suggests that any complexes formed in the drift-tube are fragmented through collisions with the buffer gas, regenerating the free NO^+ cations.

3.4. Reactions of O_2^+

Fig. 1 shows the mass spectrum of the CI reagent stream in the absence of analyte gases. Production of O_2^+ is exceptionally clean, the only significant contaminant ion being H_3O^+, which is presumably the result of residual water vapour in the apparatus.

O_2^+ has been extensively investigated as a CI reagent in SIFT-MS studies [8–14], where reaction with VOCs has been found to proceed almost entirely by charge transfer. The first ionization energy of O_2 is 12.06 eV [20], which lies above the first ionization energies of most, and well above the ionization energies of some, organic molecules. Consequently, charge transfer is likely to be fast and this is confirmed by the SIFT-MS findings. However, extensive ion fragmentation is common using O_2^+ as the CI reagent because of the large excess energy (several eV) deposited in many of the organic cations on charge transfer.

Benzene, toluene, acetonitrile and 1-butene are the only analytes that undergo non-dissociative charge transfer reactions with O_2^+. Ironically, benzene and toluene have the lowest ionization energies in the list of analytes investigated, so ionization energy differences alone are not sufficient to predict reaction outcomes. Clearly other factors will come into play, notably the energetics of bond dissociation and rearrangement processes in the parent ions.

Inspection of Table 5 confirms the expectation that ion fragmentation, with several product channels, is a common process when O_2^+ is the CI reagent. In comparison with SIFT-MS, the most frequent observation is a greater degree of fragmentation in CIRMS and a greater range of fragmentation products.

3.5. Sensitivity response of CIRMS

The response of CIRMS with respect to a certain VOC can be calculated from the instrumental conditions, fragmentation behaviour and the rate coefficient for the proton transfer reaction with H_3O^+ [1,2]. This methodology is restricted in its accuracy in respect of the uncertainty limits on the rate coefficients. Consequently, the sensitivity response of the various CI reagents to a known concentration has been assessed for a typical analyte (1-butene) at an *E/N* of 165 Td (see Section 2 for full set of conditions). This was carried out for H_3O^+, NO^+ and O_2^+, since NH_4^+ does not react with 1-butene. Using a standard gas mixture of 1-butene (1 ppmv in N_2) a series of step-wise dilutions were executed over a decade of concentration. Fig. 4 shows a correlation plot of absolute 1-butene concentration versus normalized ion count rate. All ion count rates are normalized to a nominal one million reagent ion counts following the methodology of deGouw et al. [21] and are expressed as normalized counts per second, or ncps for short. The data demonstrate the linearity of response of the instrument across a large concentration range. The derived sensitivity responses for 1-butene with H_3O^+, NO^+ and O_2^+ are $6.3_7 \pm 0.0_3$, $5.9_3 \pm 0.0_2$ and 7.8 ± 0.1 ncps ppbv^{-1} (uncertainties quoted at 1σ, the uncertainties are for H_3O^+ and NO^+ are statistically insignificant but quoted for completeness). The plots for H_3O^+ and NO^+ have zero intercepts, whereas the O_2^+ data show a small non-zero intercept with a value of +10.8 ncps, presumably arising from unwanted ions or impu-

Table 4
Product distributions from the reaction of NO^+ with a range of analytes at $E/N = 165$ Td

Compound	IE[a] (eV)	M	Product ion	*m*/*z*	Relative abundance
Acetaldehyde	10.23	C_2H_4O	$(M–H))^+$	43	77
			Not identified	41	18
			Not identified	39	2
			Not identified	27	3
Acetone	9.70	C_3H_6O	$M{\cdot}NO^+$	88	78
			$(M–(CH_3))^+$	43	22
Acetonitrile	8.72	C_2H_3N	M^+	42	87
			$(M–H){\cdot}NO^+$	71	13
Benzene	9.24	C_6H_6	M^+	78	100
1-Butene	9.55	C_4H_8	$M{\cdot}NO^+$	86	12[b]
			M^+	56	24[b]
			$(M–(H))^+$	55	2
			Not identified	44	9
			$(M–(CH_2))^+$	42	12
			$(M–(CH_3))^+$	41	2
			$(M–(C_2H_3))^+$	29	33
			$(M–(C_2H_4))^+$[c]	28	6
Ethanol	10.48	C_2H_6O	$(M–(H))^+$	45	97
			$(M–(OH))^+$	29	1[d]
			$(M–(H)–(H_2O))^+$	27	2
Ethyl acetate	10.01	$C_4H_8O_2$	$M{\cdot}NO^+$	118	4
			$(M–(C_2H_3))^+$	61	42[d]
			$(M–(CH_5O)^+$	55	1
			$(M–(C_2H_3O))^+$	45	2
			$(M–(C_2H_5O))^+$	43	51[d]
Hexanal	9.72	$C_6H_{12}O$	$(M(–H))^+$	99	3
			$(M–(C_2H_5))^+$	71	15
			$(M–(C_3H_5O))^+$	43	43
			$(M–(C_3H_5O)–(H_2))^+$	41	30
			$(M–(C_3H_5O)–((2H_2))^+$	39	3
			$(M–(C_4H_7O)–(H_2))^+$	27	5
Methacrolein	9.65	C_4H_6O	$(M(–H))^+$	69	5
			$(M–(CH_3C))^+$	43	2[d]
			$(M–(CHO))^+$	41	78[d]
			$(M–(CHO)–(H_2)–(H))^+$	39	15
Methyl benzoate	9.32	$C_8H_8O_2$	Not identified	107	2
			$(M–(CH_3O))^+$	105	88[d]
			Not identified	104	2
			Not identified	103	2
			Not identified	102	1
			$(M–(CH_3OCO))^+$	77	3
			Not identified	45	2
Methyl vinyl ketone[e]	9.65	C_4H_6O	$M{\cdot}NO^+$	100	6
			$(M–H){\cdot}NO^+$	99	7
			Not identified	98	8
			$(M–(H))^+$	69	10
			$(M–CH_3))^+$	55	30
			$(M–(C_2H_3))^+$	43	33
			$(M–(C_2H_3O))^+$	27	6
Toluene	8.83	C_7H_8	M^+	92	100

[a] From Ref. [20].

[b] Ratio of $M{\cdot}NO^+$ to M^+ is concentration dependent.

[c] Tentative assignment.

[d] Owing to water contamination, ion origin may possibly lie in fragmentation of the proton transferred parent.

[e] *Note*: dimer and dimer fragmentation removed (for details see Ref. [15]).

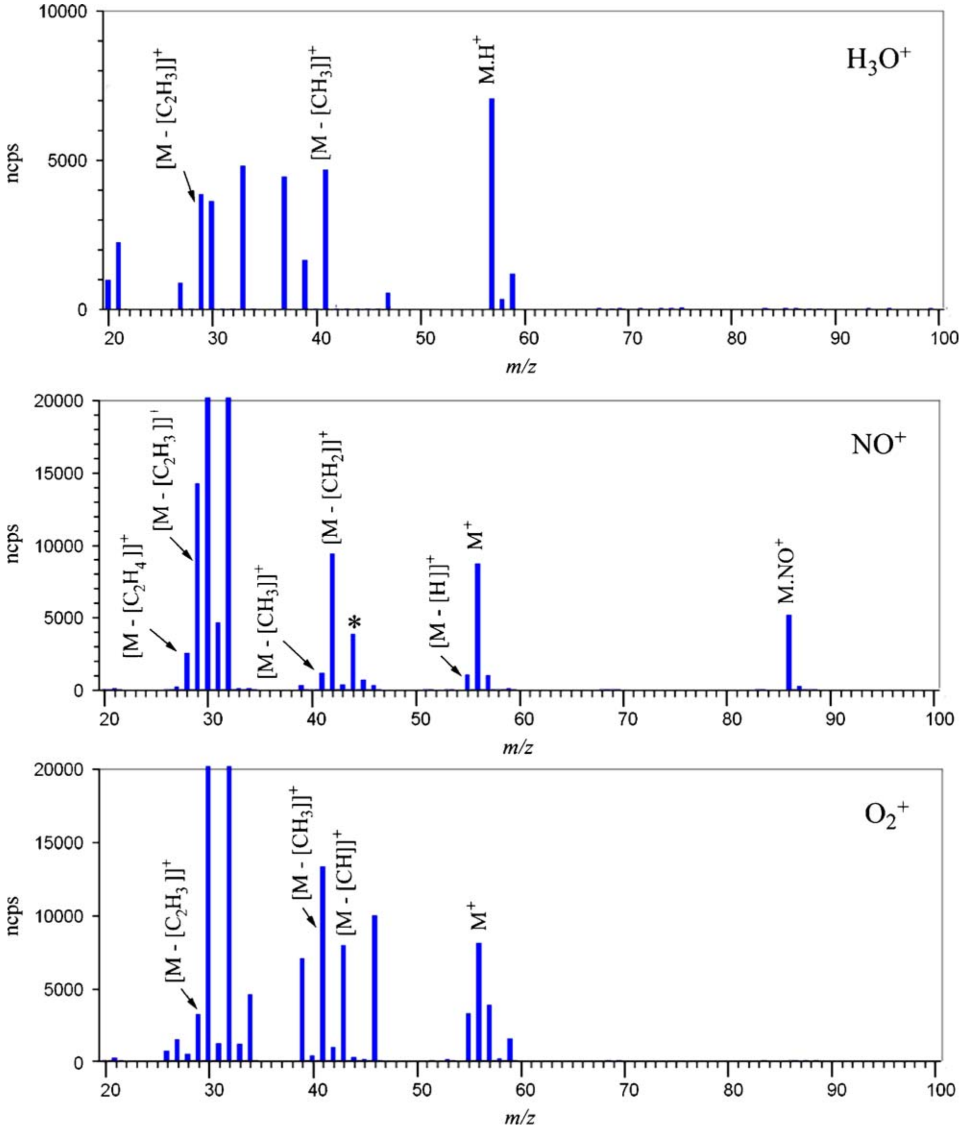

Fig. 3. Mass spectra from reaction of H_3O^+, NO^+ and O_2^+ with 1-butene. No reactions with NH_4^+ were observed. Peaks which could be due to proton transfer reactions arising from contaminant including H_3O^+ ions are marked with an asterisk.

rities. The standard deviations on the calibrations are low. It is apparent for this analyte that the sensitivity does not differ significantly with reagent ion. The absolute magnitude of the sensitivity response is lower than those, for example, reported by deGouw et al. [21], reflecting the lower reagent ion count rates as compared to those produced from a hollow cathode H_3O^+ source and the different set of experimental conditions.

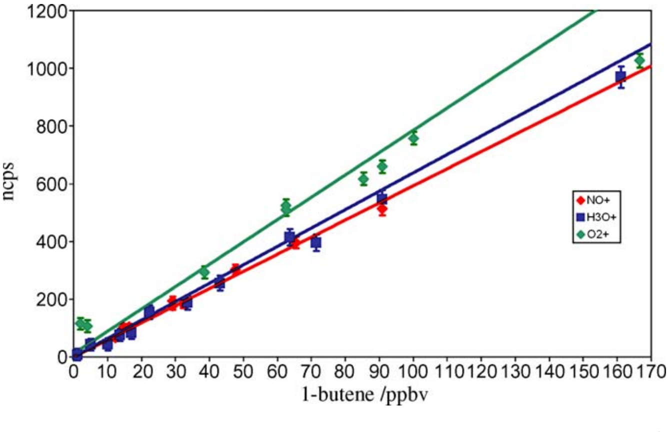

Fig. 4. Sensitivity of CIRMS to absolute concentration of 1-butene with H_3O^+, NO^+ and O_2^+.

4. Discussion

This work has demonstrated that CIRMS can build on SIFT-MS in its ability to exploit a variety of CI reagents. This can be achieved without any mass pre-selection of ions, which simplifies the experimental arrangement considerably. The ability to use a wide range of reagent ions generates a far more versatile technique than standard PTR-MS. The value of employing reagents other than H_3O^+ will depend on the system being explored and the analytical aims. We have shown elsewhere that

Table 5
Product distributions from the reaction of O_2^+ with a range of analytes[a] at $E/N = 165$ Td

Compound	M	Product ion	m/z	Relative abundance
Acetaldehyde	C_2H_4O	$(M–H)^+$	43	100
Acetone	C_3H_6O	$(M–(CH_3))^+$	43	100
Acetonitrile	C_2H_3N	M^+	41	100
Benzene	C_6H_6	M^+	78	100
1-Butene	C_4H_8	M^+	56	25
		$(M–CH))^+$	43	10
		$(M–CH_3))^+$	41	41
		$(M–C_2H_3))^+$	29	24
Ethanol	C_2H_6O	$(M–H))^+$	45	66
		$(M–(CH_3))^+$	31	34
Ethyl acetate	$C_4H_8O_2$	$(M–(C_2H_3))^+$	61	61[b]
		$(M–(CH_5O))^+$	55	5
		$(M–(C_2H_3O))^+$	45	12
		$(M–(C_2H_5O))^+$	43	22[b]
Hexanal	$C_6H_{12}O$	$(M–(H_2O))^+$	82	[c]
		$(M–(CHO))^+$	71	[c]
		$(M–(C_3H_4))^+$	60	[c]
		$(M–(C_3H_9))^+$	55	[b,c]
		$(M–(C_4H_9))^+$	43	[c]
		$(M–(C_3H_7O))^+$	41	[c]
Methacrolein	C_4H_6O	M^+	70	3
		$(M–H))^+$	69	3
		$(M–(C_2H_3))^+$	43	16[b]
		$(M–(COH))^+$	41	58[b]
		$(M–(CH_3O))^+$	39	18
Methyl benzoate	$C_8H_8O_2$	M^+	136	3
		$(M–H))^+$	135	3
		$(M–(CH_3O))^+$	105	88[b]
		$(M–(CHO_2))^+$	91	6
Methyl vinyl ketone	C_4H_6O	M^+	70	1
		$(M–H))^+$	69	18
		$(M–(CH_3))^+$	55	18
		$(M–(C_2H_3))^+$	43	47[b]
		$(M–(COH))^+$	41	10
		$(M–(C_2H_3O))^+$	27	6
Toluene	C_7H_8	M^+	92	100

[a] Only product ions with a relative abundance of >1% are listed.
[b] Cannot unambiguously be assigned to O_2^+ (cf. Table 2).
[c] Large number of fragmentation peaks, the ones listed are those with significant abundances.

one of the benefits of switching from H_3O^+ to NO^+ is that it can be used to distinguish between isobaric species on account of their different fragmentation patterns [16]. This feature may be of benefit in the speciation of simple VOC mixtures, although for complex mixtures the fragmentation may confuse rather than assist the analysis. O_2^+ offers a similar capability, although the added degree of fragmentation normally seen for this reagent may actually be detrimental to all but analysis of the simplest of VOC mixtures.

The high reactivities (essentially collision limited) seen in SIFT-MS using NO^+ and O_2^+ are reproduced for almost every molecule in the current CIRMS study. In SIFT-MS the CI reagent ions are thermalized in an inert buffer gas and thus reaction takes place at relatively low collision energies. In CIRMS the ions are dragged along the drift-tube by an electric field in order to minimize the formation of CI reagent cluster ions, which may show lower reactivity than the bare CI reagent ions.

The value of *E*/*N* is a convenient metric to describe the kinematics of a chemical ionization reaction. Here *E* is the electric field applied and *N* is the number density of the buffer molecules in the drift-tube. *E* is related to the drift velocity, vd, of an ion in the drift-tube by the relation

$$\mu = \frac{v_d}{E} \tag{3}$$

where μ is the ion mobility. The mobility is dependent on pressure and temperature and can be calculated from tabulated values of the reduced mobility μ_0, temperature *T* (in K) and pressure *p* (in Torr) from

$$\mu_0 = \frac{p}{760}\frac{273.16}{T}\mu \tag{4}$$

If the random velocity distribution of the ions in the drift-tube is taken into account then the ion kinetic energy is given by

$$\mathrm{KE_{ion}} = \frac{3}{2}k_b T + \frac{M_{\mathrm{buffer}} v_d^2}{2} + \frac{M_{\mathrm{ion}}}{2} v_d^2 \tag{5}$$

were k_b is the Boltzmann constant and M_{ion} and M_{buffer} refer to the mass of the CI reagent ion and buffer molecule, respectively. For analyte ions present in the buffer gas the available energy in the centre of mass for ion–molecule collisions [1] is given by

$$\mathrm{KE_{cm}} = \frac{M_{\mathrm{analyte}}}{M_{\mathrm{analyte}} + M_{\mathrm{ion}}}\left(\mathrm{KE_{ion}} - \frac{3}{2}k_b T\right) + \frac{3}{2}k_b T \tag{6}$$

As an example, if acetonitrile (mass 42) is the analyte in a buffer gas of air of average mass 28.8 then the collision energy between H_3O^+ and acetonitrile in the centre of mass is 0.32 eV under our experimental conditions. Under the same operating conditions, H_3O^+ + methyl benzoate (mass 106) would have a centre of mass collision energy of 0.38 eV. Therefore, over the mass range studied in this work there is <16% range in the collision energy. This additional energy, which is relatively insensitive to the mass of the analyte molecule, accounts for the increased level of fragmentation generally seen in CIRMS when compared with SIFT-MS. In addition, it accounts for the lack of association complexes between NO^+ and various organic molecules. Of course the collision energy, as defined by the ratio *E*/*N*, is a variable parameter in CIRMS and a lower value would see a reduction in fragmentation, although at the expense of increased contributions from cluster ions. We favour operation at the relatively high value of *E*/*N* of 165 Td, particularly for studies with H_3O^+ because under these conditions the formation of $H_3O^+(H_2O)_n$ clusters is negligible even when analysing very humid air.

Finally, we note that Smith and co-workers have shown using SIFT-MS that O_2^+ can be used to detect small inorganic species such as NO, NO_2 and H_2O_2 [22,23]. The proton affinities of these molecules are too low to be detected using proton transfer from H_3O^+. Thus, O_2^+ offers added value here that could also easily be exploited in CIRMS. These opportunities will be explored in a future study from our laboratory.

5. Conclusions

CIRMS has been applied for the first time to a range of VOCs with a variety of functional groups. We have shown that clean sources of H_3O^+, NH_4^+, NO^+ and O_2^+ can be generated using a radioactive ion source which is easily and rapidly switchable from one reagent to another. NO^+ and O_2^+ generally show a more complex set of ion products than the proton sources H_3O^+ and NH_4^+. Fragmentation is particularly prominent for O_2^+, where the primary mode of operation is charge transfer reaction. The findings of this work show similarities to previous extensive work carried out using SIFT-MS, although the higher collision energies employed in CIRMS do also introduce some significant differences in chemical outcomes.

The CIRMS technique offers much greater versatility than standard PTR-MS, which is almost entirely restricted to reactions of H_3O^+. This added dimension can potentially be exploited in the speciation of isobaric compounds, through the use of fragmentation ‘fingerprints’ when employing NO^+ or O_2^+. NO^+ and O_2^+ also offer opportunities to detect species which do not react with H_3O^+. Thus, CIRMS forms a powerful and highly general technique for the speciation and quantification of trace gases.

References

[1] W. Lindinger, A. Hansel, A. Jordan, Int. J. Mass Spectrom. Ion Processes 173 (1998) 191.
[2] C. Warneke, J. Kuczinski, A. Hansel, A. Jordan, W. Vogel, W. Lindinger, Int. J. Mass Spectrom. Ion Processes 154 (1996) 61.
[3] A. Amann, G. Poupart, S. Telser, M. Ledochowski, M. Schmid, S. Mechtcheriakov, Int. J. Mass Spectrom. 239 (2004) 227.
[4] A. Critchley, T.S. Elliott, G. Harrison, C.A. Mayhew, J.A. Thompson, T. Worthington, Int. J. Mass Spectrom. 239 (2004) 235.
[5] G. Harrison, A.D.J. Critchley, C.A. Mayhew, J.M. Thompson, Br. J. Anaesthesia 97 (2003) 797.
[6] T. Su, W.J. Chesnavich, J. Chem. Phys. 76 (1982) 5183.
[7] D. Smith, P. Španel, Mass Spectrom. Rev. 25 (2005) 661.
[8] P. Španel, D. Smith, Int. J. Mass Spectrom. 167/168 (1997) 375.
[9] P. Španel, D. Smith, Int. J. Mass Spectrom. 176 (1998) 203.
[10] P. Španel, D. Smith, Int. J. Mass Spectrom. 165/166 (1997) 25.
[11] D. Smith, T. Wang, P Španel, Rapid Commun. Mass Spectrom. 17 (2003) 2655.
[12] P. Španel, D. Smith, Int. J. Mass Spectrom. 172 (1998) 137.
[13] P. Španel, D. Smith, Int. J. Mass Spectrom. 181 (1998) 1.
[14] A.M. Diskin, T. Wang, D. Smith, P. Španel, Int. J. Mass Spectrom. 218 (2002) 87.
[15] K.P. Wyche, R.S. Blake, K.A. Willis, P.S. Monks, A.M. Ellis, Rapid Commun. Mass Spectrom. 19 (2005) 3356.
[16] R.S. Blake, C. Whyte, C.O. Hughes, A.M. Ellis, P.S. Monks, Anal Chem. 76 (2004) 3841.
[17] D.R. Hanson, J. Greenberg, B.E. Henry, E. Kosciuch, Int. J. Mass Spectrom. 223 (2003) 507.
[18] C. Warneke, J. deGouw, W.C. Kuster, P. Goldan, R. Fall, Environ. Sci. Technol. 37 (2003) 2494.
[19] N. Adams, L. Babcock, T. Mostefaoui, M. Kerns, Int. J. Mass Spectrom. 223 (2003) 459.
[20] NIST Chemistry Webbook, http://webbook.nist.gov.
[21] J.A. deGouw, P.A. Goldan, C. Warneke, W.C. Kuster, J.M. Roberts, M. Marchewka, S.B. Bertman, A.A.P. Pszenny, W.C. Keene, J. Geophys. Res. (2003) 108, doi:10.1029/2003JD003863.
[22] D. Smith, P. Španel, Rapid Comm. Mass Spectrom. 14 (2000) 646.
[23] P. Španel, A.M. Diskin, T. Wang, D Smith, Int. J. Mass Spectrom. 228 (2003) 269.